Dynamical Bottlenecks to Intramolecular Energy Flow

R. Paškauskas,[1,*] C. Chandre,[2] and T. Uzer[1]

[1]*Center for Nonlinear Sciences, School of Physics, Georgia Institute of Technology, Atlanta, Georgia 30332-0430, USA*
[2]*Centre de Physique Théorique - CNRS, Luminy - Case 907, 13288 Marseille cedex 09, France*

(Received 10 August 2007; published 27 February 2008)

Vibrational energy flows unevenly in molecules, repeatedly going back and forth between trapping and roaming. We identify bottlenecks between diffusive and chaotic behavior, and describe generic mechanisms of these transitions, taking the carbonyl sulfide molecule OCS as a case study. The bottlenecks are found to be lower-dimensional tori; their bifurcations and unstable manifolds govern the transition mechanisms.

DOI: 10.1103/PhysRevLett.100.083001 PACS numbers: 33.15.Hp, 34.10.+x, 82.20.Db, 82.20.Nk

Chemical reactions usually proceed through a complex choreography of energy flow processes that deliver the needed vibrational energy to the reactive mode. The manner and time in which energy travels determine the outcome of the reaction and the properties of the products. The conventional wisdom concerning this fundamental process is that vibrational energy travels very fast and, well before a reaction takes place, distributes itself statistically among the modes of the molecule, assumed to resemble an ensemble of coupled oscillators. However, there is increasing evidence that the approach to equilibrium usually proceeds more slowly than predicted by statistical theories [1]—and it is also nonuniform, showing intriguing fits and starts. This anomalous diffusion is caused by variety of phase space structures, such as resonant islands or tori that strongly slow down the trajectories passing nearby [2,3] and therefore are said to be "sticky" [4]. To date, the theories so successfully applied in pioneering works [5,6] to lower-dimensional systems have not been extended beyond 2 degrees of freedom due to severe technical difficulties [7].

In this Letter we identify a family of bottlenecks (which differ from conventional sticky structures in their lack of stability), using the OCS molecule as a case study. However, our findings are not specific to this molecule, indeed, they are not specific to molecules at all: they are applicable to all Hamiltonian systems with more than 2 degrees of freedom and "mixed" dynamics (where order and chaos coexist). The earliest investigations in this subject involved mappings, toy models, and variants of galactic Hamiltonians [4]. More recent examples from physics include the dynamical evolution of Mars-crossing asteroids [8], superradiant instabilities in atomic gases [9], and the approach to equilibrium in systems with long-range interactions [10].

Collinear (i.e., 2 degree-of-freedom) models of OCS have served as a traditional test bed for studying intramolecular dynamics in the chaotic regime [11] and these classical findings have been confirmed in parallel quantal wave packet calculations [12]. In contrast, we use a Hamiltonian involving three strongly coupled degrees of freedom, namely, two interatomic distances R_1 and R_2, and a bending angle α (with their canonically conjugate momenta P_1, P_2, and P_α). The interaction potential consists of Morse potentials for each diatomic pair and a coupling potential of the Sorbie-Murrell form [11,13]. These details aside, there is nothing special about this potential energy surface (other than being very well known). Its relevant feature is that the three modes are so strongly coupled that the system does not reduce to a lower-dimensional system, a widely shared characteristic of excited molecular systems. The computations explained below were performed at 90% of the dissociation energy of the weaker bond where a rich mixture of chaotic and regular dynamics is observed [14]. Trajectories in the vicinity of a specific periodic orbit with elliptic normal stability are studied, focusing on their escape to the chaotic region, and identifying a generic mechanism of crossover from diffusion [15] to hyperbolicity and chaos.

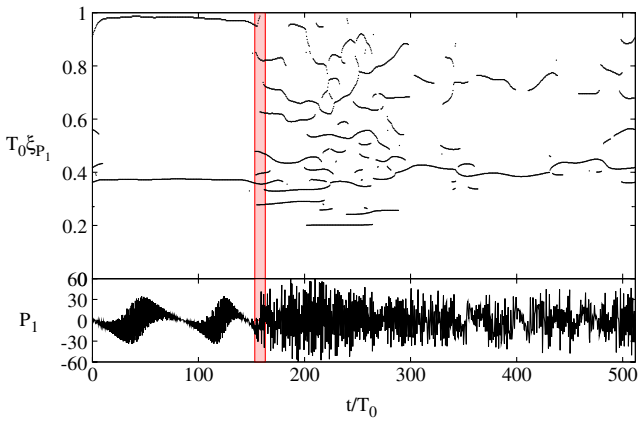

FIG. 1 (color online). The generic behavior of chaotic trajectories in Hamiltonian systems involves substantial fraction of intermittent behavior. The time-frequency analysis of a typical OCS trajectory (top panel) allows one to register the transition region (shaded band) and the frequencies ξ of the regular motion, while the time series (lower panel) display the striking features of this abrupt change. t is time (in units of $T_0 = 0.063 \times 10^{-12}$ s) and ξ_{P_1} are the frequency ridges (in units of T_0^{-1}) in the time-frequency decomposition [21] of $P_1(t)$.

Figure 1 displays the time series of such a trajectory, initially close to the periodic orbit $\mathcal{O}_a$ with period T_0 (see Ref. [14]). Figure 2 shows salient features of capture (left panel) followed by an abrupt transition to chaos (center panel). An alternative view of the transition mechanism appears in Fig. 3 in terms of the Poincaré section Σ: $P_\alpha = 0$, $\dot{P}_\alpha > 0$, $\alpha \leq \pi$. A boundary, marking the crossover from diffusion to hyperbolicity, can be identified in terms of an invariant two-dimensional torus (right panel of Fig. 2). Normal bifurcations of two-dimensional tori turn out to be the key ingredients in the transition mechanism to hyperbolicity, as will be shown below. Generically, there are two stages in the dynamics of the trajectory. During the *trapping stage* (duration t_{trap}), the trajectory is close to (quasi-)periodic, following the unstable manifold of normally hyperbolic tori with very small *positive* Lyapunov exponent (in our case, $\lambda \simeq 10^{-2}$, thus explaining the observed trapping time $t_{\text{trap}} \sim \lambda^{-1}$). During the *escape stage* (duration t_{esc}; the shaded band in Fig. 1 and "tentacles" in Fig. 3), the trajectory follows the unstable manifolds of the periodic orbit which is in 3:5 resonance with $\mathcal{O}_a$ (thick dots in Fig. 3), with a significantly larger Lyapunov exponent, leading to a fast transition to the chaotic region of phase space (center panel of Fig. 2). These two time scales usually satisfy $t_{\text{trap}} \gg t_{\text{esc}}$. Observations of repeated trapping-escape-chaotic processes in relatively short trajectory segments ($\sim 10^3 T_0$) provide evidence that these effects are prevalent. According to the dynamical systems theory, invariant structures with minimal hyperbolicity (in our case integral surfaces with small positive Lyapunov exponent) determine the main features of transients in chaotic systems. Normally hyperbolic invariant manifolds [16] have recently been implicated in the symbolic dynamics and phase space partition of higher-dimensional chaotic Hamiltonian systems [17], systems with small-dimensional saddles such as the "Crossed Fields" [18] and the Restricted Three Body Problems [19].

Using a combination of trajectory diagnostic tools like Lyapunov maps [14,20], time-frequency analysis [21], and methods from the theory of dynamical systems like periodic and quasiperiodic orbit computations [22,23], we relate the phenomenon of trapping to invariant structures in phase space and to lower-dimensional invariant tori (with a relation to their normal stability properties), in particular. It is commonly assumed that in "typical" Hamiltonian systems with a large number of degrees of freedom N, the relative measure of N-dimensional invariant tori (N local integrals) in thermodynamic limit is either zero or one [24]. The implication is that chaotic systems with large N approach conditions of the stochastic ansatz, and hence, the trapping phenomenon described above is insignificant. On the other hand, it has been established recently that high-order resonances form robust islands of secondary structures with positive measure [25].

In order to identify bottlenecks of transition from diffusion to chaos, we monitor the progress of invariant phase space structures along the transition channel using rotation numbers. The results are summarized in Fig. 4, which is central to understanding this transition. In a trapping region around the elliptic periodic orbit $\mathcal{O}_a$ (left panel of Fig. 2), the rotation numbers are obtained from the frequency map analysis [15] on the surface of section. It can be characterized by a single $\omega_{\text{trap}} \approx 0.605\,56$, implying that a two-dimensional torus is the relevant invariant structure in the trapping process. Having computed a family of two-dimensional tori, parametrized by rotation numbers ω, it is evident that ω_{trap} places the torus on the hyperbolic branch of the bifurcation diagram represented in Fig. 4. This implies that the escape is mediated by manifolds of a torus with hyperbolic normal stability. The duration of the trapping stage is approximately 150 returns on Σ, and is consistent with the maximal Lyapunov exponent $\lambda < 0.05$. Processes associated with the escape from the trapping region can be better understood by analyzing the tangent space of the elliptic periodic orbit $\mathcal{O}_a$ that locally has the structure of a direct product (center + center) $\mathbb{T} \times I_1 \times \mathbb{T} \times I_2$, with the periodic orbit at the origin. The elements of the two intervals $I_i \subset \mathbb{R}$ are rotation numbers ω_i, which

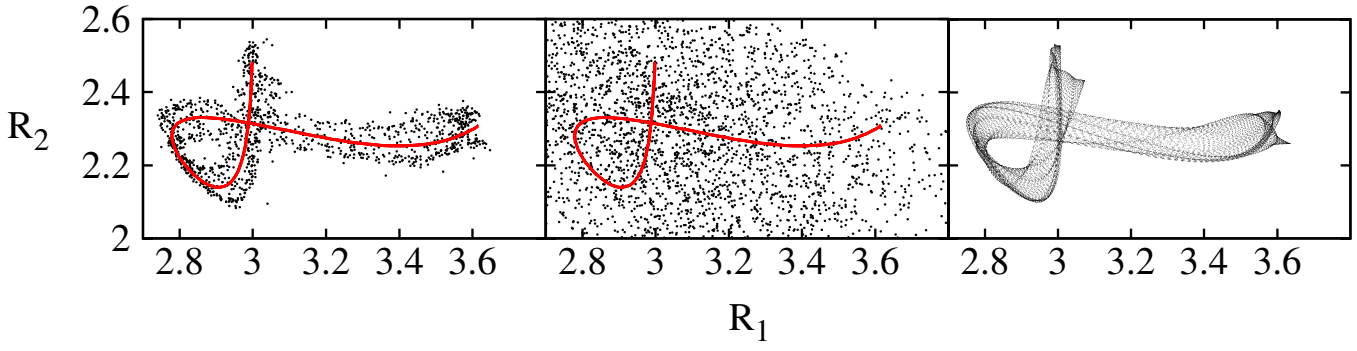

FIG. 2 (color online). Projections of the trajectory near a periodic orbit $\mathcal{O}_a$ (with period T_0), analyzed in Fig. 1. The trajectory is represented in (R_1, R_2) plots, broken down into segments, corresponding to the *trapping stage* (left panel) and chaotic stage (center panel). The bottleneck of transition from diffusion to hyperbolicity can be identified as a two-dimensional invariant torus (right panel.) The trajectory is sampled at fixed time intervals $T_0/2$. The orbit $\mathcal{O}_a$ is shown as a solid curve in the center.

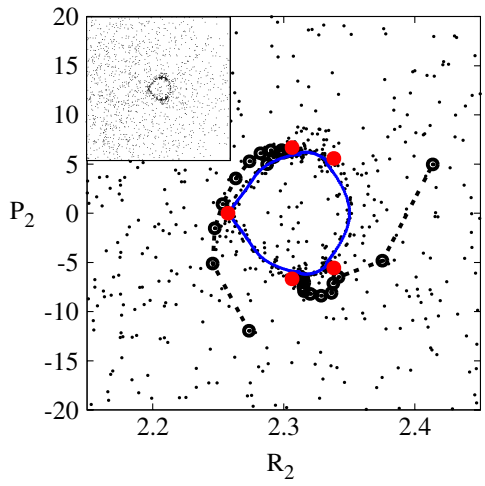

FIG. 3 (color online). Poincaré section of the trajectory near a periodic orbit $\mathcal{O}_a$, analyzed in Figs. 1 and 2. The bottleneck (a two-dimensional torus) is a loop (blue) at the bifurcation point ("D" in Fig. 4). The trajectory is trapped in the vicinity of a loop (which is clearly seen from the inset). The escape stage is shown as two "tentacles", which extend along the unstable manifolds of a resonant periodic orbit (the five red dots around the center).

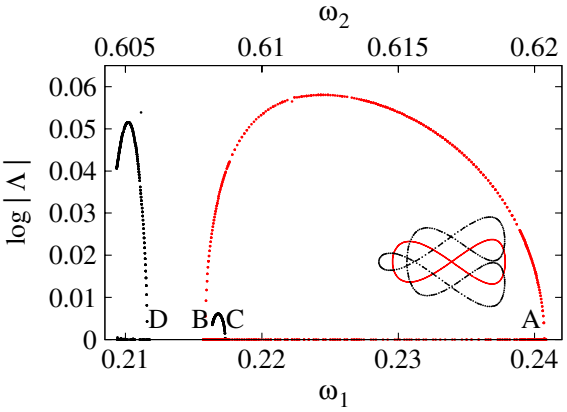

FIG. 4 (color online). Fine structure of invariant tori, scanned along the transition channel. The plot shows how Lyapunov exponents depend on the rotation number ω. The points of frequency halving bifurcations (A–D) can be interpreted as bottlenecks of transition from diffusion to hyperbolicity. Red dots: family of loops arising from the periodic orbit $\mathcal{O}_a$. Black dots: frequency halved loop, emerging at the bifurcation point A. Insets display (R_1, P_1) projections of loops near the bifurcation point A. Red: loop with elliptic normal stability and $\omega = \omega_1 \approx 0.240\,67$. Black: loop with hyperbolic normal stability and $\omega = \omega_2 = (\omega_1 + 1)/2 \approx 0.620\,33$.

are not unique in general: The choice is fixed by requiring $\lim_{\mu\to 0}\omega_i = \omega_i^0$, where μ is a measure of the "diameter" of the torus and ω_i^0 are stability angles of the periodic orbit $\mathcal{O}_a$ ($\omega_1^0 = 0.245\,006\,33$ and $\omega_2^0 = 0.370\,468\,72$). The Poincaré map induces rotations on $\mathbb{T}$, $r_{\omega_1} \times 1 \times r_{\omega_2} \times 1$, where r_ω is a rotation on $\mathbb{T}$ with the rotation number ω. Partial (or complete) resonances are determined by one (or two) resonance conditions $n\omega_1 + m\omega_2 + k = 0$, where (n, m, k) are integers such that $|n| + |m| + |k| > 0$. The most striking trapping effects are observed for partial resonances of the type $\mathbb{T} \times I_1 \times \{0\} \times \{0\}$, and $\{0\} \times \{0\} \times \mathbb{T} \times I_2$. Choosing either of the two situations, a resonance channel has been constructed by finding the two-dimensional invariant tori for $\omega_i \in I_i$. In order to find these tori we consider the Poincaré map $\mathcal{F}_\Sigma$: $\Sigma \mapsto \Sigma$. The sections of two-dimensional invariant tori are one-dimensional closed curves (called hereafter "loops"). We consider loops as discretizations of γ: $\mathbb{T} \mapsto \Sigma$(with periodic boundary condition $\gamma(s) = \gamma(s + 1)$) and require that the Poincaré map $\mathcal{F}_\Sigma$, restricted to the loop is equivalent to a rigid rotation r_ω. This translates into an invariance condition:

$$\mathcal{F}_\Sigma(\gamma(s)) = \gamma(s + \omega). \tag{1}$$

Tori may have hyperbolic normal linear stability, therefore a search for them cannot rely on methods exploiting "stickiness" properties. Equation (1) is solved using damped Newton iterations for the Fourier coefficients of $\gamma(s)$. The linear stability properties of the loop are determined by (Λ, ψ), solutions of the generalized eigenvalue problem:

$$D\mathcal{F}_\Sigma(s)\psi(s) = \Lambda\psi(s + \omega). \tag{2}$$

Equation (2) has a one-dimensional kernel, which we eliminate using singular value decomposition. At the periodic orbit, $D\mathcal{F}_\Sigma$ has two pairs of complex eigenvalues $\exp[\pm\imath\omega_i^0]$ ($i = 1, 2$).

The set of two-dimensional tori is found to be discontinuous at the gaps in Fig. 4 due to complete resonances (periodic orbits) and secondary invariant structures. Normal stability is typically elliptic for small $|\omega - \omega_i^0|$. We identify the two-dimensional invariant torus at the period doubling bifurcation point as a bottleneck of a given resonance channel. The rationale follows from the theory of dynamical systems: Beyond the bifurcation point at $\omega = \omega^c$, the normal stability changes to hyperbolic. This change affects trajectories passing by its neighborhood. One recurrent observation is that the continued fraction expansion of bifurcation rotation numbers has a tail composed of small integers (see Table I). This feature is reminiscent of the observation that the continued fraction

TABLE I. Rotation numbers of the two-dimensional invariant tori at the bifurcation points A, B, C, D shown in Fig. 4.

ω	Value	Cont. frac.
ω_A^c	0.240 711 317 575	[4, 6, 2, 11, 5, 5…]
ω_B^c	0.215 852 976 389	[4, 1, 1, 1, 2, 1, 1, 1, 1, 2, 1, 1…]
ω_C^c	0.608 654 398 762	[1, 1, 1, 1, 4, 45, 1, 1, 1, 1…]
ω_D^c	0.605 804 087 926	[1, 1, 1, 1, 6, 3, 2, 2, 1…]

expansion of the frequency of the last invariant torus in generic Hamiltonian systems with 2 degrees of freedom is noble (with a tail of ones) in many situations [5].

The signature of sticky regions in mixed systems are long-time correlations which decay slower than exponential (usually according to a power law) [3]. The slowing down of exponential separations due to trapping has been documented for the collinear model of OCS [26]. For a quantum-mechanical system close to dissociation (like this molecule) longer-than-statistical lifetimes mean that the spectral line widths associated with excitations will be narrower than expected. Indeed, the photoabsorption linewidths will be affected, and their narrowing should be detectable.

In this Letter we identified a single family of phase space structures which is at the source of the uneven flow of vibrational energy. We explained a paradoxical situation, namely, that integral surfaces with *positive* Lyapunov exponents (i.e., unstable) can trap chaotic trajectories. These surfaces are closely connected with local integrals and partial resonances (and the number of isolating integrals [27]) in realistic chaotic Hamiltonian systems with many degrees of freedom. In this sense, these structures found here differ from the conventional sticky (marginally stable, or ''elliptic'') tori. Widespread observations of repeated trapping-escape-chaotic processes in short trajectory segments provide evidence that our findings are generic and occur frequently in many settings ranging from plasmas to celestial mechanics. For example, the complex mass transport processes by which asteroids reach the inner solar system proceed in a manner practically identical to the vibrational energy flow described here: Long quiet periods with little change are followed by bursts of rapid and chaotic change, which raise the asteroid's eccentricity enough to cross the orbits of terrestrial planets [28]. This correspondence is seen particularly clearly in the time-frequency analysis of asteroid motion [29]. Other examples are afforded by systems with long-range interactions, like free-electron lasers or atoms in optical cavities. Recent numerical simulations on a particular model show that the system remains in quasistationary states (QSS, associated with regular behavior) for a long time and then escapes from these QSS to find its way to equilibrium [10]. The close similarity of the behavior of these systems and Fig. 1 implies that analysis in terms of phase space structures will be fruitful in those situations also.

This research was partially supported by the U.S. National Science Foundation. C. C. acknowledges support from Euratom-CEA (Contract No. EUR 344-88-1 FUA F).

*rytis@gatech.edu

[1] See, e.g., articles in the Special Issue, Chaos **15**, No. 1 (2005).
[2] G. M. Zaslavsky, *Hamiltonian Chaos and Fractional Dynamics* (Oxford University, Oxford, 2005).
[3] C. F. F. Karney, Physica (Amsterdam) **8D** 360 (1983).
[4] G. Contopoulos, *Order and Chaos in Dynamical Astronomy* (Springer, Berlin, 2002).
[5] M. J. Davis, J. Chem. Phys. **83**, 1016 (1985).
[6] C. C. Martens, M. J. Davis, and G. S. Ezra, Chem. Phys. Lett. **142**, 519 (1987).
[7] R. E. Gillilan and G. S. Ezra, J. Chem. Phys. **94**, 2648 (1991).
[8] Ch. Froeschlé, G. Hahn, R. Gonczi, A. Morbidelli, and P. Farinella, Icarus **117**, 45 (1995).
[9] S. Slama, S. Bux, G. Krenz, C. Zimmermann, and Ph. W. Courteille, Phys. Rev. Lett. **98**, 053603 (2007).
[10] Y. Y. Yamaguchi, J. Barré, F. Bouchet, T. Dauxois, and S. Ruffo, Physica (Amsterdam) **337A**, 36 (2004).
[11] D. Carter and P. Brumer, J. Chem. Phys. **77**, 4208 (1982).
[12] L. L. Gibson, G. C. Schatz, M. A. Ratner, and M. J. Davis, J. Chem. Phys. **86**, 3263 (1987).
[13] A. Foord, J. G. Smith, and D. H. Whiffen, Mol. Phys. **29**, 1685 (1975).
[14] E. Shchekinova, C. Chandre, Y. Lan, and T. Uzer, J. Chem. Phys. **121**, 3471 (2004).
[15] J. Laskar, Physica (Amsterdam) **67D**, 257 (1993).
[16] M. W. Hirsch, C. C. Pugh, and M. Shub, *Invariant Manifolds* (Springer, New York, 1977).
[17] R. de la Llave (private communication).
[18] T. Uzer, C. Jaffé, J. Palacián, P. Yanguas, and S. Wiggins, Nonlinearity **15**, 957 (2002).
[19] G. Gomez, W. S. Koon, M. W. Lo, J. E. Marsden, J. Masdemont, and S. D. Ross, Nonlinearity **17**, 1571 (2004).
[20] C. Froeschlé, E. Lega, and R. Gonczi, Celestial Mechanics and Dynamical Astronomy **67**, 41 (1997).
[21] C. Chandre, S. Wiggins, and T. Uzer, Physica (Amsterdam) **181D**, 171 (2003).
[22] C. Simó, in *Modern Methods of Analytical Mechanics and their Applications* in CISM Courses and Lectures, Vol. 387, edited by V. V. Rumyantsev and A. V. Karapetyan (Springer, New York, 1998).
[23] À. Jorba, Nonlinearity **14**, 943 (2001).
[24] C. Froeschlé, Astrophys. Space Sci. **14**, 110 (1971).
[25] A. Haro and R. de la Llave, Phys. Rev. Lett. **85**, 1859 (2000).
[26] M. J. Davis, Chem. Phys. Lett. **110**, 491 (1984).
[27] G. Contopoulos, L. Galgani, and A. Giorgilli, Phys. Rev. A **18**, 1183 (1978).
[28] A. Morbidelli, Celestial Mechanics and Dynamical Astronomy **73**, 39 (1999).
[29] T. A. Michtchenko and D. Nesvorny, Astron. Astrophys. **313**, 674 (1996).